

# Complex Dual Tree Wavelet Multi-Level Feature Based Transformation Parameter Estimation for 3d Medical Image Registration

P.H.Sunitha, Sreerama Reddy G.M, Cyril Prasanna Raj

**Abstract:** 3D image registration of CT and MRI data is carried out using DTCWT sub bands by considering the features from all 64 bands. The features are selected by considering Mattes Mutual Information Metric and the optimizer algorithm estimates the optimum transformation parameters from all the 64 bands. Transformation parameters from eight low pass bands from each octave are averaged to identify optimum registration parameters. Similarly, for registration of high pass bands mean of transformation parameters from 56 bands are identified. The proposed registration algorithm is suitable for register multimodal medical images and the proposed algorithm is validated for more than 20 3D images. Mutual information and joint entropy is estimated to demonstrate the advantages of proposed algorithm over that of intensity based algorithm. With features identified from 56 bands with six orientations the registered image is found to consist of features from both input images with closeness level measured to be within 12%.

**Index Terms:** Image registration, 3D, Complex Dual Tree Wavelet, Multilevel, Medical Image

## I. INTRODUCTION

With advances in medical imaging technologies in 3D visualization of anatomy, detection and monitoring of tumors has given edge over existing technologies for doctors in treating patients. More than 40 3D images and 20 different structures are analyzed in patient treatment. Determining the tumors avoiding critical structures, knowing the patterns of tumors, motions and changes in motions during course of treatment is time consuming and demands highly accurate registration techniques of multimodal images. The medical equipment used in clinical workflow need to be integrated with 3D/4D registration techniques considering all uncertainties, breathing motion, respiration sorting and in-room imaging. The objects in medical images change with time due to elasticity and abnormalities leading to motion of objects in all three directions that are captured in 3D images. Wavelets have been predominantly used for feature extraction, however with limitations such as shift invariance and directional selectivity issues, complex tree wavelets are being used in place of wavelet transforms. Dual Tree Complex Wavelet Transforms that generate twice large number of sub bands compared with wavelet transforms,

selection of appropriate sub bands that contain the required features for image registration determines image registration accuracy. In [1] author has reported on use of Dual Tree Complex Wavelets as pre-processing module by using filters that are near shift invariant and have directional selectivity. The advantages of complex wavelets are that it has low redundancy and complex for pre-processing. The wavelet sub bands obtained by complex dual tree wavelets are robust for changes in contrast of the two images and have local means that provide information for alignment of phase information considering wavelet coefficients. With large amount of motion observed in medical images during data acquisition, both the global motions as well as local motions are extracted from multiple sub bands captured at various resolutions. In 3D registration, registration should be carried on every slice of 3D data set as there could be non-uniform movement in the structures due to non-rigid objects and removal or changes in objects due to clinical intervention [2][3]. In Image registration, the deformed images is transformed by a transformation factor of T that is computed by considering the distance between features such as edges, points and regions [4] that are present in the deformed and reference image. In [5] Registration of MRI and CT images by selection of tibia and femur features from the binary images and affine transformation, validation of the algorithm is carried out by considering correlation coefficient. In [6], preprocessing techniques such as geometric feature based segmentation dynamic threshold method, feature extraction techniques such as automated trunk slices extraction and transformation technique like multithread iterative closest point are used for registration. Validation metrics such as negative normalization correlation and Euclidean distance error are computed for registering PET and CT images. In [5], phase information coefficients are considered to align images by using Dual Tree Complex wavelet transforms (DTCWT) coefficients. The shift invariance property of the front end filter along with directional selective property available in DTCWT bands the registration algorithm becomes robust to local mean and contrast changes in images. In [7], two step registration processes is carried out by considering the sub band information computed using DTCWT. Coarse level registration is carried out by considering edges and cross correlation function from low frequency bands and the registration is improved by considering mutual information from six orientation bands. In [8],

**Revised Manuscript Received on July 05, 2019.**

P.H.Sunitha, Research scholar, M.S.Engineerig college, Bangalore.

Sreerama Reddy G.M, Principal, Department of Electronics and communication ,CBIT,Kolar.

Cyril prasanna Raj P, Professor, Department of Electronics and communication, M.S .Engineerig college, Bangalore.

Retrieval Number: H7331068819/19©BEIESP  
DOI:10.35940/ijitee.H7331078919

Published By:  
Blue Eyes Intelligence Engineering  
& Sciences Publication



registration of medical images is carried out by computing DTCWT sub bands for key point's selection, Hausdorff distance for similarity measurement between key points and Niche particle swarm optimization for affine transformation. Evaluation metrics such as correlation coefficient, normal mutual information, mean square error and time are used. Most of the methods discussed use affine transformation as deformation model, feature selection and similarity checking based on mutual information. Accuracy in registration algorithm depends on selection of object function and transformation model. In [9][10][11][12], to improve the registration accuracy gradient information is combined with mutual information to capture similarities in both images. For 3D registration along with gradient in x and y directions it is also required to determine gradient in z direction. Along with gradient information, orientation of objects and their edges when combined with mutual information can further improve registration accuracy. For the registered images metrics such as cross correlation, mean square and PSNR are used as performance measurement metrics. It is also required to consider the transformation parameters as one of the metrics for registration. In this work, gradient information and orientations in the gradients are computed by use of 3D DTCWT and the transformation parameters are used to evaluate the performances of proposed 3d image registration algorithm. Image fusions of 3D medical images have been carried out in [13] considering DTCWT features and matching these wavelet features based on statistical mapping approaches. The major properties of complex wavelets sub bands is the interoperability of sub bands such that by interpolation of each of the complex wavelet sub bands the sub bands of shifted data can be obtained. With direction information available in the sub bands, change in direction will result in linear phase change hence providing additional parameter for feature matching in registration. Using dual tree complex wavelet for 3D data registration will lead to complexity in processing algorithms as the 3D transformation will generate both real and imaginary sub bands. There is a need for novel and robust algorithms that process the real and imaginary sub bands for performing accurate registration of 3D data that is faster and less complex in data processing.

## II. DTCWT

DTCWT are complex wavelet coefficients, supporting shift invariance and directional choice along six orientations. The filters in DTCWT are of Hilbert pair of bases  $\psi_h$  and  $\psi_g$ , satisfying  $\psi_g(t) = H(\psi_h(t))$ . DTCWT is a complete transform with redundancy (2m:1, for m-dimensional signals) and has demonstrated superior results for image processing as compared with DWT [14][15]. 3D DTCWT is defined as  $\psi(x, y, z) = \psi(x)\psi(y)\psi(z)$ , where  $\psi(x)$ ,  $\psi(y)$  and  $\psi(z)$  are complex wavelets represented by  $\psi(x) = \psi_h(x) + j \psi_g(x)$ ,  $\psi_h$  and  $\psi_g$  are real and imaginary wavelet transforms. The real part of  $\psi(x, y, z)$  represented by  $\psi_a = \text{Real}\{\psi(x, y, z)\} = \psi_1(x, y, z) - \psi_2(x, y, z) - \psi_3(x, y, z) - \psi_4(x, y, z)$  (where  $\psi_1, \psi_2, \psi_3$  and  $\psi_4$  are 3D wavelet bases and are separable) containing 1(Wavelet Sub Band)  $WSB_{lsb}$  and 7  $WSB_{hsb}$ . The remaining sub bands are computed by considering complex conjugation. Equation (1) represents the orthonormal combination matrix

of DTCWT computed using DWT trees. Considering Eq. 1, there are four low pass sub bands and 28 high pass sub bands with each of these bands having unique spatial orientation and motion information [16].

The 3D DTCWT structure is shown in Fig. 1(a). The first stage is the 2D DTCWT processor comprising of two stages and the third stage is the processor in temporal domain. 3D input data comprising of 52 frames with each frame of size 512 x 512 is processed simultaneously by 52 numbers of 2D DTCWT processing unit. Every 2D frame (represented by  $S^1(Z_1Z_2)$ ) is processed row wise first and then column wise in the 2D processor generating four sub bands from each frame. The third stage DTCWT processor processes the sub bands in the z-direction to generate eight sub bands thus representing the first octave bands (shown in Fig.1(c)). Similarly, the 3D DTCWT structure generates eight octaves with each octave consists of eight sub bands of one  $WSB_{lsb}$  and seven  $WSB_{hsb}$ .

The 2D DTCWT processor comprises of two stage processing unit, the row processing and column processing. The row processing stage consists of four filter banks represented by {H<sub>oa</sub>, H<sub>ob</sub>, H<sub>1a</sub> & H<sub>1b</sub>}, each of these filter outputs are further processed by four column filters. The sub bands of high pass ( $D_{1a/b}^m$ ) and low pass ( $C_{1a/b}^1$ ) of 3D DTCWT are mathematically represented as in Eq. (1), where A and B are real and imaginary filter coefficients respectively.

$$C_{1a/b}^1(Z_1Z_2Z_3) = (2^j \downarrow) \left[ (A_a^j(Z_1) \pm iA_b^j(Z_1)) (A_a^j(Z_2) + iA_b^j(Z_2)) (A_a^j(Z_3) + iA_b^j(Z_3)) S(Z_1Z_2Z_3) \right]$$

(1a)

$$D_{1a/b}^1(Z_1Z_2Z_3) = (2^j \downarrow) \left[ (A_a^j(Z_1) \pm iA_b^j(Z_1)) (B_a^j(Z_2) + iB_b^j(Z_2)) (A_a^j(Z_3) + iA_b^j(Z_3)) S(Z_1Z_2Z_3) \right]$$

(1b)

$$D_{2a/b}^1(Z_1Z_2Z_3) = (2^j \downarrow) \left[ (B_a^j(Z_1) \pm iB_b^j(Z_1)) (A_a^j(Z_2) + iA_b^j(Z_2)) (B_a^j(Z_3) + iB_b^j(Z_3)) S(Z_1Z_2Z_3) \right]$$

(1c)

$$D_{2a/b}^1(Z_1Z_2Z_3) = (2^j \downarrow) \left[ (B_a^j(Z_1) \pm iB_b^j(Z_1)) (B_a^j(Z_2) + iB_b^j(Z_2)) (B_a^j(Z_3) + iB_b^j(Z_3)) S(Z_1Z_2Z_3) \right]$$

(1d)

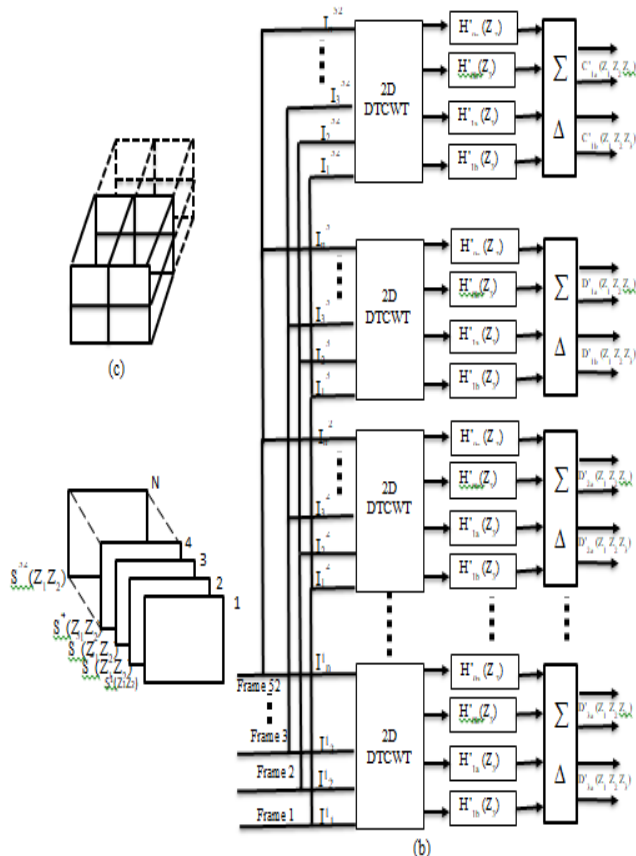


Fig. 1 DTCWT structure (a) 3D input image (b) 3D DTCWT (c) First octave of DTCWT

### III. PROPOSED REGISTRATION ALGORITHM

In image registration proposed algorithm, the dual tree complex wavelet filter of 10-tap coefficients is used to decompose unregistered image of CT and MRI into wavelet sub bands. The image registration is carried out by processing eight octave bands. For Registration, one low pass band(3DLMRI) and 7 high pass bands (3DHCT) out of 64 sub bands of DTCWT decomposition are considered. The Low Sub Band (L SB) and High Sub Band (HSB).The proposed image registration process for one octave DTCWT sub bands is shown in Fig. 2 are first processed to map the coordinates of the sub bands from local coordinates (LCS) to global coordinates (GCS) denoted by  $\{RL_{MRI}, RH_{MRI}, RL_{CT}, RH_{CT}\}$ . The inbuilt MATLAB function “imregtform” is used to compute the transformation parameters by providing information on  $\{3DL_{MRI}, RL_{MRI}, 3DL_{CT}, RL_{CT}$  and transformation type} The imregtform function requires input parameters that are initialized with MMI metric, initial radius, maximum iterations and growth factor. The function processes the input data considering the constrains and initial parameters set to compute the optimum transformation parameters. The transformation parameters T is computed from both the low pass and high pass DTCWT sub bands. From the transformation parameters obtained from all low pass bands, the average parameter is computed, and from the 56transformation parameters computed from high pass sub bands the mean of them is considered as the transformation parameters represented as  $\{3DL_{CT1}, 3DL_{CT2}, 3DL_{CT3}, 3DL_{CT4},$

$3DL_{CT5}, 3DL_{CT6}, 3DL_{CT7}, 3DL_{CT8}\}$  and 56 sub bands  $\{3DH_{CT1}, 3DH_{CT2}, \dots, 3DH_{CT56}\}$  are transformed by considering  $TP_{LAVG}$  and  $TP_{HMEAN}$ , 64 sub bands are obtained by invoking “imwarp” MATLAB function that is transformed by cogitating MRI data as reference. The 64 sub bands organized, the registered CT 3D images are obtained from computing inverse DTCWT. The reference MRI 3D image and the registered 3D CT image are compared to evaluate the performance of the proposed algorithm.



Fig. 2 Proposed 3D image registration algorithm

In 3D image registration technique, the positions of row, column and frame of the 3D images are computed first in terms of global coordinate system. The global reference positions of both MRI and CT images are identified. The transformation parameters are computed by matching the intensity levels of MRI and CT image. This step is iterative and is repeated until best transformation matrix is obtained by setting the optimization and matching metric. Matching metric is either mutual information (Butz and Thiran, 2001, Phim et al 2003, Plumin et al, 204, Maes et al, 2003) or mean square error algorithm. Woods in 1992 introduced the Mates mutual registration measure for multimodality images based on Shannon entropy and probability of co-occurrence measure. Mattes algorithm works better if the matching is carried out on images with features instead of intensities. The drawback of mutual information metric for 3D image registration is the dependence of neighboring pixel in computing entropy is ignored. Transforming the input 3D image into DTCWT sub bands and considering the low pass band for registration the spatial



information from neighbouring voxels is improved [17]. The Mattes Mutual Information (MMI) metric represented by  $I(A,B)$  for DTCWT sub bands are computed as in Eq. (2),

$$I(A, B) = H(A) - H(B|A) = H(B) - H(A|B) \quad (2)$$

Where,  $H(B|A) = - \sum_{a,b} p(a, b) \log p(b|a) = H(A, B) - H(A)$ , represents the conditional entropy which is computed by considering the average of the entropy of image sub band B for each of the intensity in sub band A.  $H(A)$  and  $H(B)$  (shown in Eq. (3)) represents the individual image entropies of image A and image B, with  $p_A^T$  and  $p_B^T$  representing marginal probability distributions.

$$H(A) = - \sum_a p_A^T(a) \log p_A^T(a) \quad \forall A(x_A) = a | x_A \in \Omega_{A,B}^T$$

$$H(B) = - \sum_b p_B^T(b) \log p_B^T(b) \quad \forall B^T(x_A) = b | x_A \in \Omega_{A,B}^T \quad (3)$$

MMI is computed only by considering relationship between individual voxels in 3D image, with use of DTCWT sub bands MMI computed also considers spatial information. Variable voxels sizes are considered to compute MMI from each of the DTCWT sub bands with localized orientations. For low pass bands voxel size is set to  $8 \times 8 \times 8$  as the spatial relationships between frames is considered and for high frequency bands voxels size is set to  $16 \times 16 \times 16$  as the orientations in six directions are considered.

Optimization is the process of identifying the maximum or the minimum similarity measure between two images. Mathematically defined as  $\min D [MRC^1_{1a/b}, T(CTC^1_{1a/b})]$ , where T is the transformation function. The optimizer metric based on gradient descent (Balci et al 2007, Tang et al 2006) is defined by  $Match (MRI, CT) = \frac{\text{SumMRIC}T}{\sqrt{(\text{SumMRI} \cdot \text{SumCT})}}$ , where  $\text{SumMRIC}T = \text{MRI}(\text{index}) \cdot \text{CT}(\text{index})$  and all other terms similarly defined. From the transformation parameters  $(T = T_{all} = [T_{scale}][T_{shear}][T_{RotZ}][T_{RotX}][T_{RotY}][T_{Reflex}])$  determined as represented in Eq. (4), the MRI data is transformed to obtain the registered image with respect to CT image.

$$T = \begin{bmatrix} a & d & g & p \\ b & e & h & q \\ c & f & i & r \\ j & m & n & s \end{bmatrix} = \begin{bmatrix} \cos\alpha & \sin\alpha & 0 & 0 \\ -\sin\alpha & \cos\alpha & 0 & 0 \\ 0 & 0 & 1 & 0 \\ 0 & 0 & 0 & 1 \end{bmatrix} \begin{bmatrix} \cos\beta & \sin\beta & 0 & 0 \\ -\sin\beta & \cos\beta & 0 & 0 \\ 0 & 0 & 1 & 0 \\ 0 & 0 & 0 & 1 \end{bmatrix} \begin{bmatrix} \cos\gamma & 0 & -\sin\gamma & 0 \\ 0 & 1 & 0 & 0 \\ \sin\gamma & 0 & \cos\gamma & 0 \\ 0 & 0 & 0 & 1 \end{bmatrix} \begin{bmatrix} -1 & 0 & 0 & 0 \\ 0 & -1 & 0 & 0 \\ 0 & 0 & -1 & 0 \\ 0 & 0 & 0 & 1 \end{bmatrix}$$

(4)

Where, p, q, r represents perspective transformation, parameters a to i represents linear transformation of Scaling, Shear, Rotation, parameters k, l, m represent translation along X, Y and Z axis and s is Scaling.

IV. RESULTS AND DISCUSSION

For evaluation of Image registration algorithm standard data sets from Vanderbilt University with prior permission

from Creative Commons, 171 Second Street, Suite 300, San Francisco, California, 94105, USA that comprises of 20 sets of MRI and CT data with 52 frames per 3D data is considered for analysis. The MRI (fixed data) and CT (moving data) is transformed into DTCWT sub bands considering 10-tap symmetric filter coefficient and the low pass sub bands of fixed image and moving image are presented in Fig. 3 and Fig. 4 respectively for frames 1, 4 and 8.

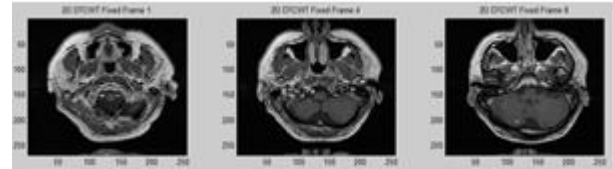


Fig. 3 DTCWT sub bands of MRI data of frame 1, 4 and 8

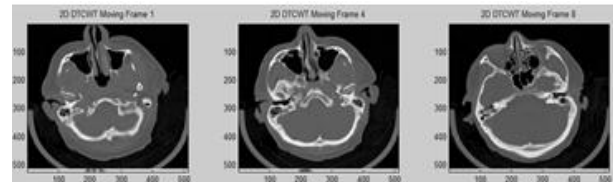


Fig. 4 DTCWT sub bands of CT data of frame 1, 4 and 8

From 3D input images considered for registration, it is observed that the intensity, orientation, position and size of objects and regions vary frame to frame. These variations can be considered as features in the DTCWT sub bands need to be captured, compared and corresponding transformation parameters need to be computed for registration. 3D DWT sub bands exhibit checker board errors if there are edges other than vertical and diagonal edges. The advantages of DTCWT is that the checker board errors that are observed in DWT sub bands do not occur in DTCWT sub bands as each sub band contains an image pattern with spatial orientation, motion direction that are localized in sub bands. In order to estimate redundancy between 3D data frames the first frame and consecutive second frame of MRI and CT are considered and joint histograms are computed are presented in Fig. 5. Similarity is observed between consecutive MRI data frames and CT data frames as indicated by the joint histogram with gray shades. Considering first frame of MRI and first frame of CT and computing joint histogram, it is found that the gray shades are scattered indicating limited redundancy between these frames. The purpose of registration is to improve redundancy between these frames and all consecutive frames.

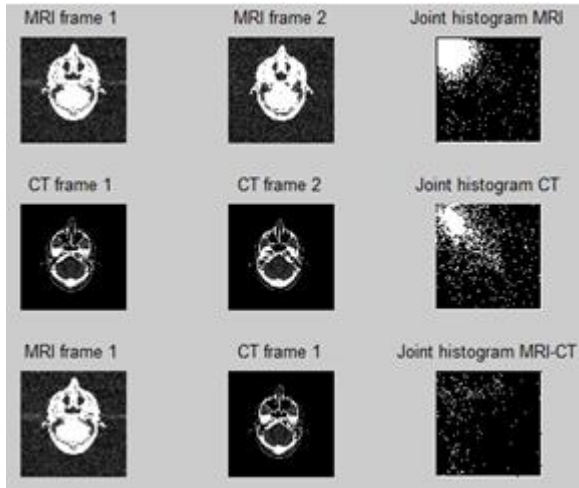


Fig. 5 Joint histogram of CT and MRI images

As registration is carried out in wavelet domain, joint histogram of DTCWT bands of MRI and CT data prior to registration are computed and presented in Fig. 6. As DTCWT sub bands localize the features in an image in various sub bands, the redundancy between MRI and CT data as observed in Fig.5 will be distributed in DTCWT sub bands. The low pass bands joint histogram (figure titled “joint histogram MRI-CT” in Fig. 6a) indicates that there are very few gray regions and thus redundancy is limited. Similarly the “joint histogram MRI-CT” title figure in Fig. 6b presents joint histogram of one of the high frequency bands of MRI and CT with very few regions of gray areas.

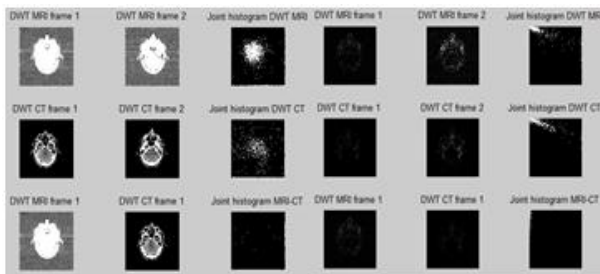


Fig. 6 Joint histogram of DTCWT (a) WSB<sub>Low</sub> pass sub band (b) WSB<sub>High</sub> pass sub band

From the results presented in Figure 6, the redundancy in information content in the consecutive sub bands of both MRI and CT are localized in multiple sub bands. As observed in the joint histogram of MRI-CT sub bands of low pass and high pass the information is distinct and each sub band holds unique features. The redundancy in information in spatial domain is combined as compared with DTCWT sub bands. Considering these distinct features in every DTCWT sub band, 3D image registration is carried out.

#### 4.1 Test Procedures

With initial translation parameters set, MRI data is translated and compared with CT data by considering Mattes mutual information metric. Optimum transformation parameters are achieved with gradient descent algorithm with multiple iterations. The transformation parameters such as scaling, rotation and translation obtained from one quadrant of DTCWT sub bands ( WSB<sub>LLL</sub>, WSB<sub>LLL</sub>, WSB<sub>LHL</sub>, WSB<sub>LHH</sub>, WSB<sub>HLL</sub>, WSB<sub>HLH</sub>, WSB<sub>HHL</sub>, WSB<sub>HHH</sub> ) are presented in Fig.7

to Fig. 9 and is compared with transformation parameters obtained from input images without DTCWT decomposition. The transformation parameters for each of the sub band are computed independently by comparing the MMI metric and gradient optimizer. For one quadrant of DTCWT sub band 24 scaling parameters, 48 rotational parameters and 24 translation parameters are obtained along the x, y and z directions.

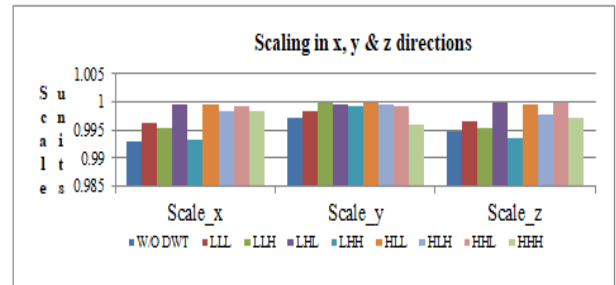


Fig.7 Optimum scaling parameters for registration

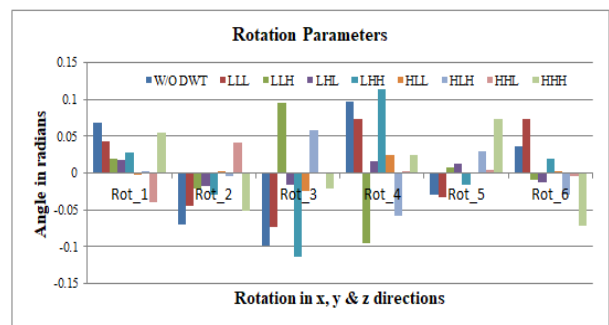


Fig. 8 Optimum rotation parameters for registration

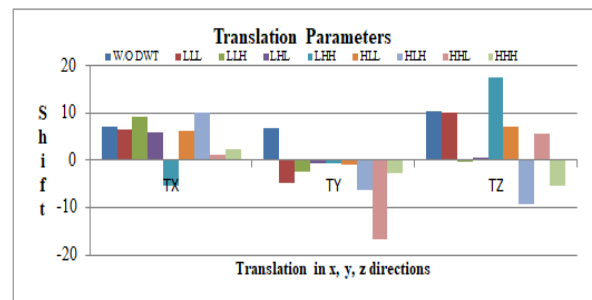


Fig. 9 Optimum translation parameters for registration

Fig.10 and Fig. 11 presents the gray scale version of eight low pass sub bands that have been obtained after 3D DTCWT representing eight quadrants information. MMI is estimated by processing the corresponding MRI and CT low pass bands and the transformation parameters are estimated.

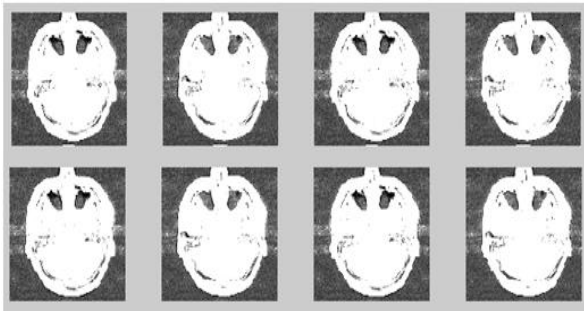


Fig. 10 Eight low pass bands of 3DTCWT output of MRI data

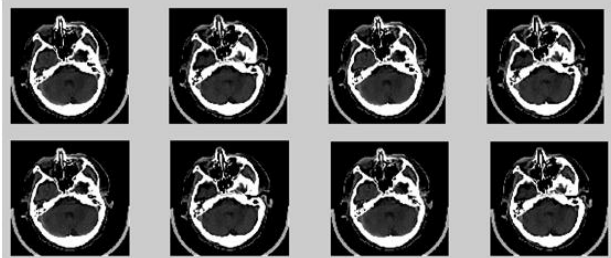


Fig. 11 Eight low pass bands of 3DTCWT output of CT data

From the transformation parameters obtained from each of the eight quadrants, mean of the transformation parameters is computed from high pass bands are considered for registration of high pass sub bands. The averages of transformation parameters are considered for registration of low pass bands. Fig. 12 presents the average scaling parameter obtained by computing MMI and optimization process. With each of the eight sub bands of CT data are transformed along the X, Y and Z directions as per the scaling parameter the registration process is accurate and is localized.

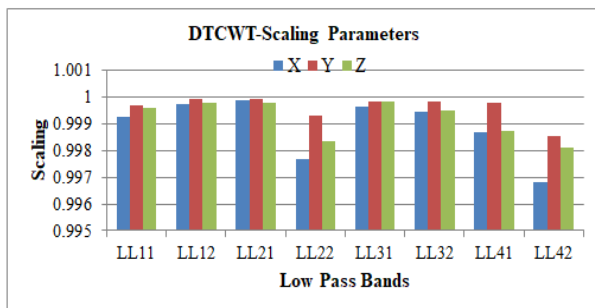


Fig. 12 DTCWT scaling parameters of low pass bands

Similarly, the rotational and translation parameters are obtained for each of the low pass bands. For the high pass bands the mean of transformation parameters are obtained and each of the CT data sub bands are transformed using these parameters. The low pass sub band and the high pass sub bands of CT data are transformed using optimum parameters.

#### 4.2 Test Results

The algorithm for image registration is developed in MATLAB and the algorithm is improved for optimization in image registration metrics and transformation parameter estimation. In proposed algorithm validation is carried out from more than 100 test 3D images of 20 patients. The data sets consist of CT and MRI images of 52 frames each of 512 x 512 sizes. Image pixel size is 0.45 units and 0.86 units for each frame of CT image and MRI image respectively along

both directions and is represented using signed number 16-bit. For analysis the registered images visual presentation both in time domain and wavelet domain are presented. After registration, the objects in MRI and CT are aligned and are clearly observed with color changes in the images. The registration results of CT and MRI data of frame 1 in wavelet domain by considering the low pass bands is illustrated in Fig.13

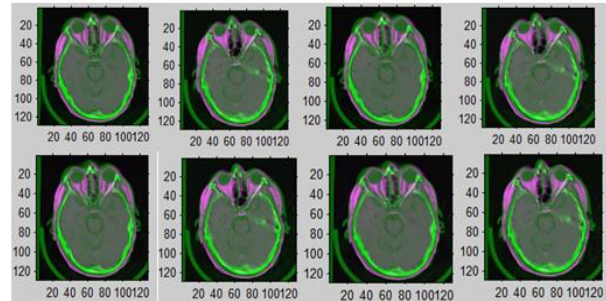


Fig.13 Low pass bands registration results

The image registration results in time domain is shown in Fig.14. Registration is carried out using intensity information of input images, DWT and DTCWT based registration algorithm. Observing Fig. 14c representing DTCWT based registration, the information in the registered image are significant and the features are more prominent as compared with the features obtained in the registered image using DWT.

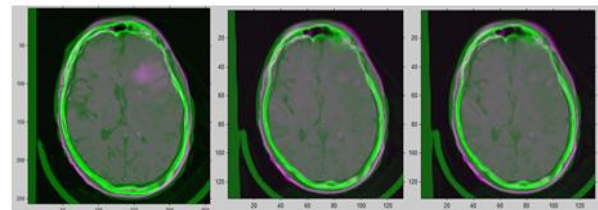


Fig. 14 Registration Results (a) Intensity (b) With DWT (c) With DTCWT

Fig.15 presents the comparison results of image registration using DTCWT and DTCWT with optimum feature selection algorithm for one frame of 3D image. From the results the visual perception of improved registration algorithm is superior compared with DTCWT based direct algorithm. As there are 52 frames in each 3D image, it is required to evaluate the registration process by considering individual frames. Fig.16 presents the joint histogram of 1<sup>st</sup> and 4<sup>th</sup> frame of registered 3D image with proposed DTCWT algorithm. Fig.17 presents the joint histogram of 1<sup>st</sup> and 4<sup>th</sup> frame with intensity based registration. Joint histogram is computed between input image CT and MRI, MRI and Registered CT, CT and Registered CT image considering all frames



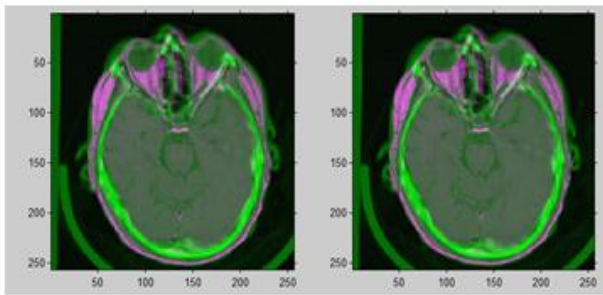


Fig.15 Comparison (a) Direct registration (b) Improved registration algorithm

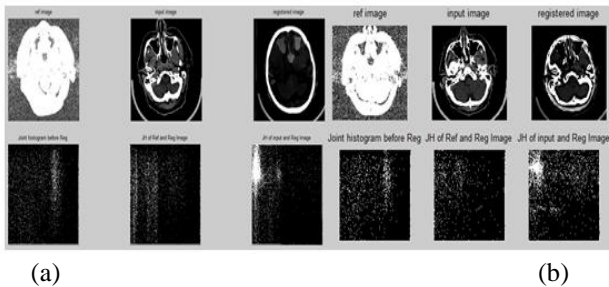


Fig. 16 Registration using proposed algorithm (a) Frame 1 (b) Frame 4

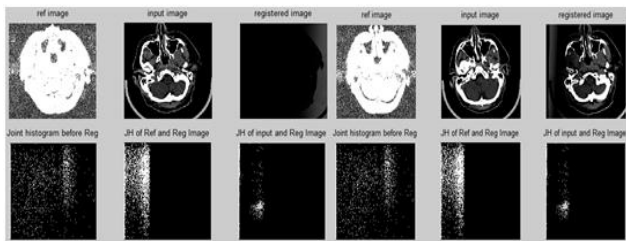


Fig. 17 Intensity registration results (a) Frame 1 (b) Frame 4

The images in first row (from left to right) is the CT, MRI and Registered CT image, the images in second row are joint histogram between CT & MRI, MRI & Registered CT, CT and Registered CT images. Comparing images and joint histogram results in Fig. 16 and Fig.17 it is found that after registration the gray area spread in the joint histogram between MRI & Registered CT, CT and Registered CT in improved and is better in DTCWT based registration algorithm.

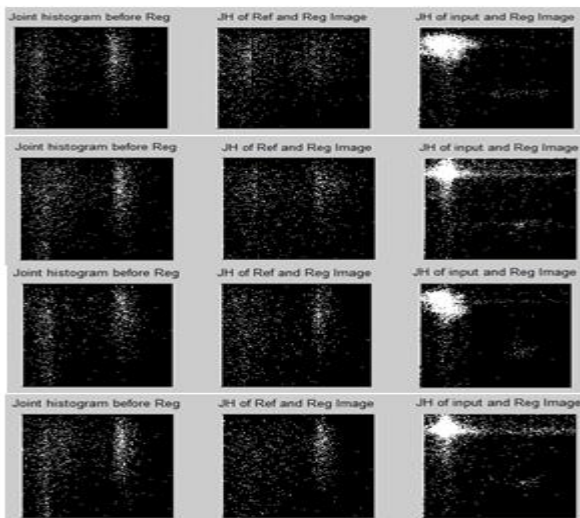


Fig.18 Comparisons of JH (a) Frame 20 (b) Frame 32

Fig.18 presents the joint histogram comparison of frame 20 and frame 32, first row representing joint histogram computed using DTCWT based algorithm and second row using intensity based algorithm. Table 1 presents the comparison of mutual information and joint entropy results obtained using intensity based 3D registration algorithm and proposed algorithm computed for 4 frames of input data.

Table 1 Comparison of metrics

Frame	Data Sets	Mutual Information (Intensity)	Mutual Information (DTCWT)	Joint Entropy (Intensity)	Joint Entropy (DTCWT)
Frame 1	CT-MRI	-0.5428	-0.5052	7.5125	7.4757
	MRI-REG	-2.2605	-0.3668	6.0370	7.4753
	CT-REG	-1.4292	0.4671	5.2058	6.6414
Frame 4	CT-MRI	-0.5909	-0.5909	7.6193	7.6193
	MRI-REG	-0.0316	-0.8405	8.3192	7.5097
	CT-REG	1.0634	0.3294	7.2243	6.3397
Frame 20	CT-MRI	0.3128	0.3128	7.7625	7.7625
	MRI-REG	0.7943	0.7462	7.9347	7.9585
	CT-REG	1.0170	1.0028	7.7120	7.7018
Frame 32	CT-MRI	-0.6157	-0.6157	7.7921	7.7921
	MRI-REG	0.0607	0.1780	7.9648	8.1622
	CT-REG	1.1875	1.3226	6.8380	7.0176

The results from Table 1 represents the mutual information registered images and joint entropy metrics are found to be closer to both the input images CT and MRI thus indicating that the registered image contains information from both the input images. The MI and JE metrics for proposed algorithm exhibits closeness in metrics as compared with intensity based metrics. In order to further improve Image registration results can be further improved by decomposing the low sub bands into higher levels by computing level 2 and level 3 decomposition and features are selected from pyramids of DTCWT sub bands.

## V. CONCLUSION

In this work, image registration is carried out by considering DTCWT sub bands. 3D DTCWT is applied on the input image data and 64 sub bands are obtained of which 56 of them hold directional information in six orientations both in real and imaginary bands. The eight low pass hold the intensity levels. The proposed algorithm for image registration evaluates the matching criterion considering all orientations and estimates optimum transformation parameters. Based on the optimum parameters estimated registration is carried out in the DTCWT sub band and the registered image is obtained. Metrics such as joint entropy and mutual information is computed to identify the impact of proposed image registration algorithm. From the obtained results, there is an improvement of over 15% in features between reference image and registered image. This improvement of more than 15% is achieved as all the six orientations are considered for image registration. The proposed algorithm is suitable for medical image processing applications and computer guided surgery.

## REFERENCES

1. Huizhong Chen, Student Member, IEEE, and Nick Kingsbury, Member, IEEE, Efficient Registration of Nonrigid 3-D Bodies, Ieee Transactions On Image Processing, January 2012 ,Vol. 21, Issue. 1,pp.262-272.
2. Y. P. Shen, "Review of image registration methods for medical images," Chinese Journal of Medical Physics, vol. 30, no. 1, pp. 3885–3889, 2013.
3. M. Toews and W.M. Wells III, "Efficient and robust model-to-image alignment using 3D scale-invariant features," Medical Image Analysis, vol. 17, no. 3, pp. 271–282, 2013.
4. F. P.M.Oliveira and J. M. R. S. Tavares, "Medical image registration: a review," Computer Methods in Biomechanics and Biomedical Engineering, vol. 17, no. 2, pp. 73–93, 2014
5. B J.Zheng,Z. Ji, K. Yu,Q.An, Z. Guo, andZ.Wu, "A feature-based solution for 3D registration of CT and MRI images of human knee," Signal, Image and Video Processing, vol. 9, no. 8, pp. 1815–1824, 2015.
6. Zhiying Song,1 Huiyan Jiang,1 Qiyao Yang,1 Zhiguo Wang,2 and Guoxu Zhang, A Registration Method Based on Contour Point Cloud for 3D Whole-Body PET and CT Images, Hindawi BioMed Research International, Volume 2017, Article ID 5380742, 11 pages.
7. Milad Ghantous, Somik Ghosh, Magdy Bayoumi , A MULTI-MODAL AUTOMATIC IMAGE REGISTRATION TECHNIQUE BASED ON COMPLEX WAVELETS
8. Jingjie Zheng · Zhenyan Ji · Kuangdi Yu · Qin An · Zhiming Guo · Zuyi Wu, A feature-based solution for 3D registration of CT and MRI images of human knee, DOI 10.1007/s11760-014-0660-5.
9. H. Rivaz, Z. Karimaghloo and D. L. Collins, "Self-similarity weighted mutual information: A new nonrigid image registration metric," Med. Image Anal., vol. 18, no. 2, pp. 343-358, Feb. 2014.
10. C. Studholme, C. Drapaca, B. Iordanova and V. Cardenas, "Deformation-based mapping of volume change from serial brain MRI in the presence of local tissue contrast change," IEEE Trans. Med. Imag., vol. 25, no. 5, pp. 626-639, May 2006.
11. D. Loeckx, P. Slagmolen, F. Maes, D. Vandermeulen and P. Suetens, "Nonrigid image registration using conditional mutual information," IEEE Trans. Med. Imag., vol. 29, no. 1, pp. 19-29, May 2010
12. M. P. Heinrich, M. Jenkinson, M. Bhushan, T. Matin, F. V. Gleeson, J. M. Brady and J. A. Schnabel, "MIND: modality independent neighbourhood descriptor for multi-modal deformable registration," Med. Image Anal., vol. 16, no. 7, pp. 1423-1435, Oct. 2012.
13. Arati Kushwaha, Ashish Khare, Om Prakash, Jong-In Song, Moongu Jeon, 3D Medical Image Fusion using Dual Tree Complex Wavelet Transform, International Conference on Control, Automation and Information Sciences, October 29-31, 2015, Changshu, China.
14. I. Selesnick and K. Y. Li, "Video denoising using 2D and 3D dual-tree complex wavelet transforms," in Wavelets: Applications in Signal and Image Processing X, vol. 5207 of Proceedings of SPIE, pp. 607–618, San Diego, Calif, USA, August 2003.
15. Selesnick, R. G. Baraniuk, and N. C. Kingsbury, "The dualtree complex wavelet transform," IEEE Signal Processing Magazine, vol. 22, no. 6, pp. 123–151, 2005.
16. Video Coding Using 3D Dual-Tree Wavelet Transform BeibeiWang,1 Yao Wang,1 Ivan Selesnick,1 and Anthony Vetro2, Hindawi Publishing Corporation EURASIP Journal on Image and Video Processing Volume 2007, Article ID 42761, 15 pages.
17. E. Shannon, "A mathematical theory of communication," Bell System Technical Journal, vol. 27, pp. 379–423/623–656, 1948

## AUTHORS PROFILE



**Mrs. SUNITHA P H**, received BE (Eln.) Mysore university, M.Tech (IE.) degree from Visvesvaraya Technological University, Belagavi, Karnataka, India. Currently, pursuing Ph.D degree from Visvesvaraya Technological University ,Belagavi, Karnataka, India. she is working as Associate Professor in Electronics and Communication Engineering Dept. M S Engineering College, Bangalore. Her current interest of research VLSI and Image Processing.



**Dr. SREERMA REDDY G.M.**, is graduated B.E in 1990 from Govt. P.D.A College of Engineering, Gulbarga, Gulbarga University, Masters from U.V.C.E. University College of Engineering, Bangalore, Bangalore university and Ph.D from J.N.T. University, Ananthapuram, Andhra Pradesh, INDIA. He is presently working as a Principal , in C.Byregowda Institute of Technology, Kolar, Karanataka, INDIA. His areas of interest are Micro Electronics/Low power VLSI/DSD, Design and FPGA of high speed low power digital up converter for power line communication systems, FACTS and power quality improvement in distribution systems.



**Dr. CYRIL PRASANNA RAJ P**, has qualified BE in ECE from SJCE, Mysore (1996). M.Tech in industrial electronics from KREC, Surarthkal, Karnataka (1999) and Ph.D. from Coventry University, UK in VLSI Signal Processing (2011). He has 12 patents and more than 50 publications. He has 16 years of experience in research. He is the current Dean (R&D) and Professor at M S Engineering College. He is in charge of R&D activities at MSEC, involved in industrial collaborations, research collaborations and career development training.